ACS Infectious Diseases

Article

pubs.acs.org/journal/aidcbc

Acinetobactin Isomerization Enables Adaptive Iron Acquisition in *Acinetobacter baumannii* through pH-Triggered Siderophore Swapping

Justin A. Shapiro and Timothy A. Wencewicz*

Department of Chemistry, Washington University in St. Louis, One Brookings Drive, St. Louis, Missouri 63130, United States

Supporting Information

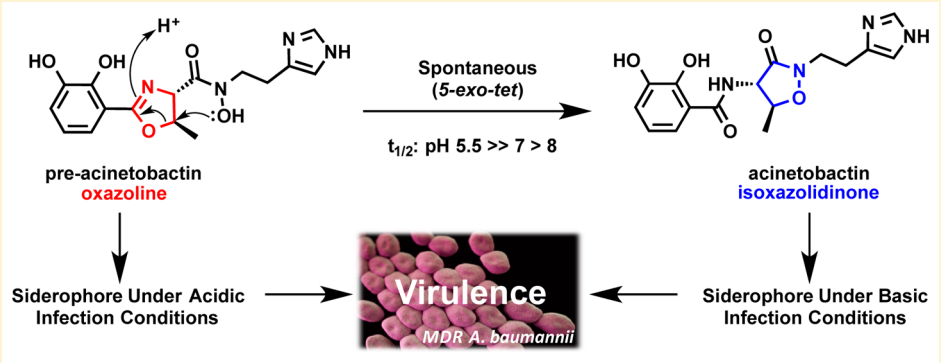

ABSTRACT: Pathogenic strains of *Acinetobacter baumannii* excrete multiple siderophores that enhance iron scavenging from host sources. The oxazoline siderophore pre-acinetobactin undergoes an unusual non-enzymatic isomerization, producing the isoxazolidinone acinetobactin. In this study, we explored the kinetics, mechanism, and biological consequence of this siderophore swapping. Pre-acinetobactin is excreted to the extracellular space where the isomerization to acinetobactin occurs with a pH-rate profile consistent with 5-*exo-tet* cyclization at C5′ with clean stereochemical inversion. Pre-acinetobactin persists at pH <6, and acinetobactin is rapidly formed at pH >7, matching each siderophore's pH preference for iron(III) chelation and *A. baumannii* growth promotion. Acinetobactin isomerization provides two siderophores for the price of one, enabling *A. baumannii* to sequester iron over a broad pH range likely to be encountered during the course of an infection.

KEYWORDS: *siderophore, acinetobactin, Acinetobacter baumannii, antibiotic resistance, antivirulence*

Multi-drug-resistant (MDR) Gram-negative bacterial pathogens represent some of the most challenging cases of health-care-associated infections.[1,2] The Center for Disease Control and Prevention (CDC) lists MDR *Acinetobacter* strains as a serious threat with 7300 of the ∼12 000 annual nosocomial infections being entirely resistant to at least three classes of frontline antibiotics (63% MDR rate).[3] Clinical isolates of MDR *A. baumannii* are routinely resistant to all or nearly all FDA-approved antibiotics, with one outbreak strain in China harboring a plasmid containing 45 antibiotic resistance genes.[4] The rising threat of MDR *A. baumannii* has increased clinical use of polymixins,[5] largely abandoned due to nephrotoxicity, and inspired the search for new, nontraditional therapeutics including antivirulence strategies.[6,7] Interruption of iron acquisition systems is an attractive antivirulence approach for targeting *A. baumannii*.[8−12] Most highly virulent strains produce a cocktail of three siderophores, small-molecule iron(III) chelators,[13] to scavenge iron from the host, which maintains extremely low free iron(III) levels (10^{-24} M in human serum) as a form of innate resistance.[14,15] The *A. baumannii* siderophore cocktail typically includes acinetobactin,[16] fimsbactin,[17] and baumannoferrin.[18] Acinetobactin is a firmly established virulence factor in mouse infection models[19] and is highly conserved in the genomes of >50 *A. baumannii* clinical isolates.[11]

Acinetobactin was first reported in 1994 as **1a** containing a methyl oxazoline heterocycle (Figure 1A).[16] Gene clusters and other essential genes encoding acinetobactin biosynthesis enzymes (*entA*, *basABCDEFGHIJ*), efflux a.k.a. "release" proteins (*barAB*), and uptake/utilization proteins (*bauABCDE*) have been annotated and functionally characterized in non-pathogenic and highly virulent strains (Scheme S1).[20−25] Aldrich and co-workers used this knowledge to launch a successful campaign developing small-molecule inhibitors of acinetobactin biosynthesis targeting BasE, which activates 2,3-dihydroxybenzoic acid as an acyl adenylate.[10,26] In 2009, Walsh and co-workers showed that acinetobactin and related siderophores pseudomonine[27] and anguibactin[28] (Figure 1B,C) are biosynthesized on homologous nonribosomal peptide synthase (NRPS) modular assembly lines.[23,24] Walsh and co-workers

Received: December 7, 2015
Published: December 9, 2015

DOI: 10.1021/acsinfecdis.5b00145
ACS Infect. Dis. 2016, 2, 157−168

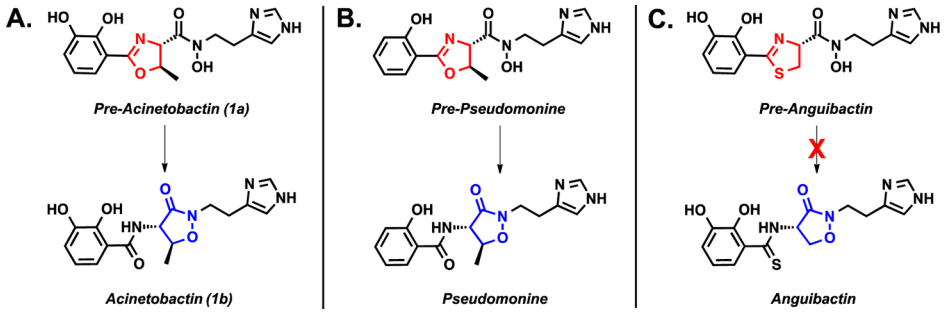

Figure 1. Isomerization of siderophores in the acinetobactin family. Pre-acinetobactin (A) and pre-pseudomonine (B) isomerize at pH 8 from oxazoline (red heterocycle) to isoxazolidinone (blue heterocycle). Pre-anguibactin (C) is locked in thiazoline form (red heterocycle).

Scheme 1. Synthesis of Pre-acinetobactin TFA Salt (1a·TFA), Acinetobactin TFA Salt (1b·TFA), and Corresponding Iron(III) Complexes (Structure Unknown)

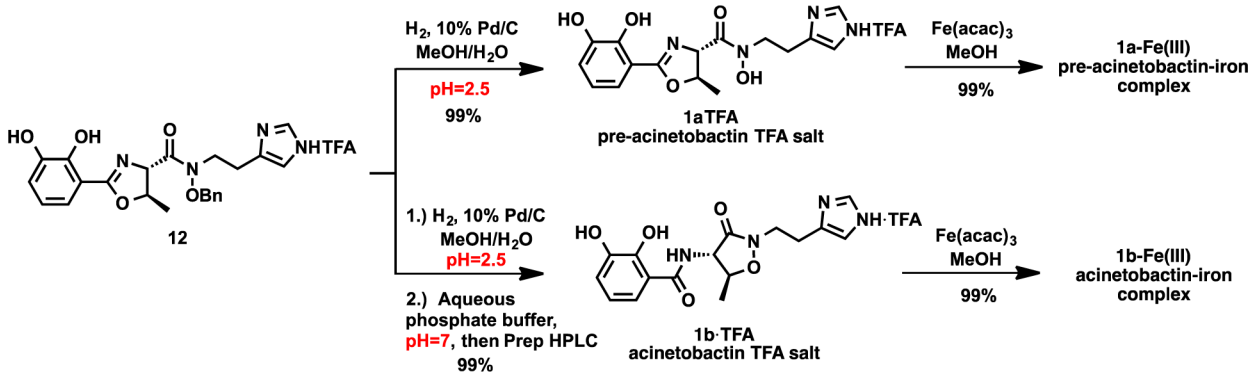

were the first to definitively report that acinetobactin is produced in a "pre" form **1a** containing an oxazoline heterocycle (Figure 1A) and is then released from the NRPS after attack of *N*-hydroxyhistamine on the thioester carbonyl of the penultimate enzyme-linked biosynthetic intermediate (Scheme S1). At pH 8, pre-acinetobactin, **1a**, rapidly isomerizes non-enzymatically to acinetobactin, **1b** (Figure 1A). The NMR spectra of enzymatically produced **1b** matched the reported spectra from the original isolation paper,[16] thus correcting this misconception in the literature and firmly establishing acinetobactin **1b** as the isomer present at pH ∼8.[24]

Pre-pseudomonine, a siderophore produced by some Pseudomonads,[27] differs from pre-acinetobactin only by the hydroxylation state of the phenyl ring. Walsh and co-workers found that pre-pseudomonine undergoes an analogous post-biosynthetic isomerization reaction at pH ∼8 to produce pseudomonine (Figure 1B). A third member of this siderophore class, pre-anguibactin, differs from pre-acinetobactin and pre-pseudomonine in that it is built from L-cysteine, instead of L-threonine, producing a thiazoline heterocycle compared to the oxazoline heterocycles of pre-acinetobactin and pre-pseudomonine. Unlike pre-acinetobactin and pre-pseudomonine, pre-anguibacin does not isomerize at pH 8 and is locked in as the thiazoline-containing isomer (Figure 1C).[24] Pre-anguibactin has been rigorously characterized as a functional siderophore for *Vibrio anguillarum*,[29] and a crystal structure of pre-anguibactin bound to gallium(III) has been solved.[30] Studies with pre-anguibactin suggest that the "pre" form of this siderophore class is biologically relevant and demands investigation of both pre-acinetobactin **1a** and acinetobactin **1b** as contributors in *A. baumannii* iron acquisition.

Acintobacter baumannii pathogens are capable of growth over a wide pH range with most sites of infection being acidic.[2,31] We hypothesized that the isomerization of pre-acinetobactin **1a** would be faster if the hydroxamic acid (pK_a ∼ 9) nucleophile was partially deprotonated. Therefore, we predicted that the isomerization of pre-acinetobactin **1a** to acinetobactin **1b** would be slower at acidic pH, favoring pre-acinetobactin **1a** as the major isomeric form of the siderophore present at acidic *A. baumannii* infection sites. To test our hypothesis, we probed the kinetics and mechanism of acinetobactin isomerization and established a pH-rate profile of the reaction over a pH range of 5.5−8.0. We also probed the role of pH on iron(III) chelation and *A. baumannii* growth promotion. Our studies suggest a role for both acinetobactin siderophore isomers in *A. baumannii* iron acquisition during the course of an infection, reshaping our chemical understanding of these important virulence molecules in a relevant biological context.

RESULTS AND DISCUSSION

Synthesis and Isolation of Acinetobactin. A total synthesis by Takeuchi and co-workers was adapted to produce the key intermediate benzyl-protected pre-acinetobactin **12** and is described in the Supporting Information (Scheme S2). In previous chemical synthesis[32] and biosynthesis[24] studies with acinetobactin, no method was reported for stabilizing and storing pre-acinetobactin **1a**. We found that the TFA salt of pre-acinetobactin **1a** was stable in methanol (pH ∼2) after hydrogenolysis of benzyl-protected precursor **12** (Scheme 1). Performing the same benzyl deprotection reaction and subsequently adjusting to pH 7 provided acinetobactin **1b** in quantitative yield. Standardized solutions of **1a** TFA salt and **1b** were prepared in deuterated methanol spiked with an

DOI: 10.1021/acsinfecdis.5b00145
ACS Infect. Dis. 2016, 2, 157−168

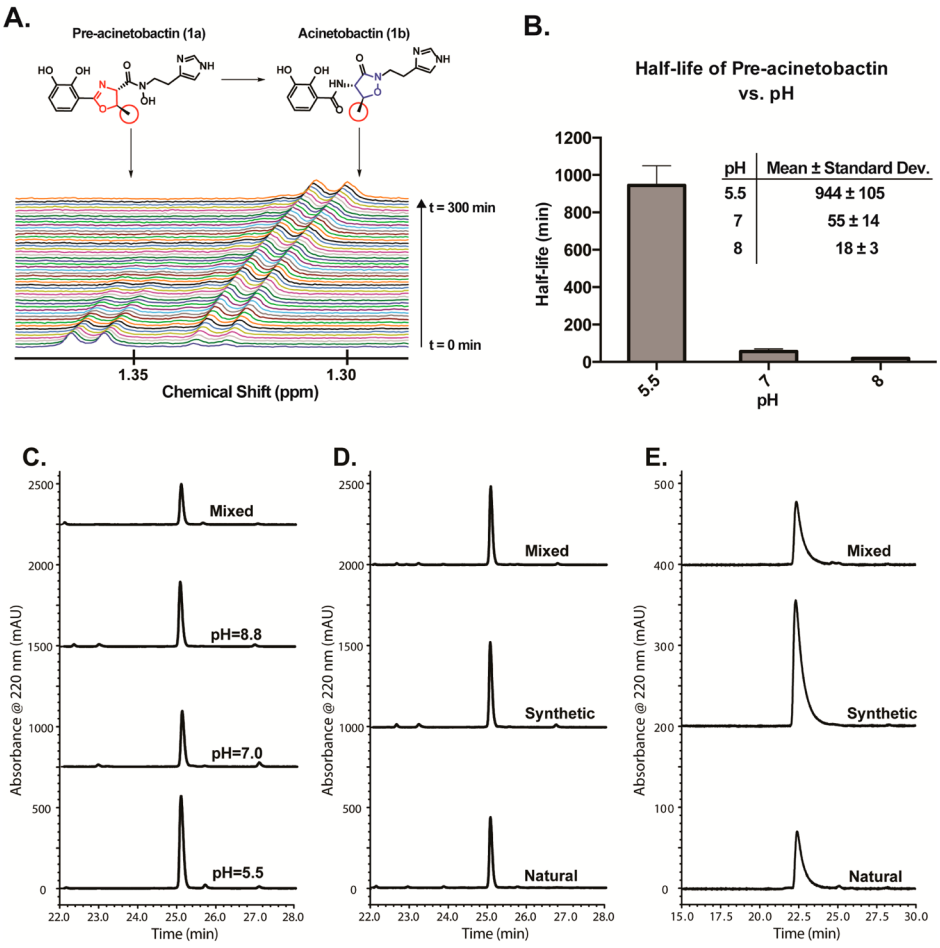

Figure 2. (A) Representative ^{1}H NMR kinetic study of the first-order isomerization of pre-acinetobactin to acinetobactin at pH 7, 27 °C in 10% D_2O/90% H_2O. (B) Half-lives of pre-acinetobactin at pH 5.5, 7.0, and 8.0 at 27 °C, with error bars showing standard deviation. (C) C18 HPLC analysis of acinetobactin from isomerization of pre-acinetobactin at pH 5.5, 7.0, and 8.0. (D) C18 HPLC analysis of natural acinetobactin isolated from *A. baumannii* and synthetic acinetobactin produced at pH 5.5, 7.0, and 8.0. (E) Chiral HPLC analysis of natural and synthetic acinetobactin (mixture of samples generated at pH 5.5, 7.0, and 8.0).

acetonitrile internal standard and were stable at −80 °C for >1 year. All characterization data of **1b** matched a natural analytical standard of acinetobactin **1b** isolated from fermentation of *A. baumannii* ATCC 17978 (Table S3). We report the first detailed 2D NMR characterization of pure pre-acinetobactin **1a** TFA salt (Table S2). Iron complexes of pre-acinetobactin, **1a-Fe(III)**, and acinetobactin, **1b-Fe(III)**, were prepared by treating methanolic solutions of iron-free siderophores, **1a** and **1b**, with tris(acetylacetonato) iron(III). The structure of these complexes is still unknown, but **1a-Fe(III)** (λ = 515 nm, magenta solution) and **1b-Fe(III)** (λ = 570 nm, purple solution) form stable, unique iron(III) complexes as determined by UV−vis and MS−MS. This synthetic route provides efficient access to both acinetobactin isomers and is amenable to the synthesis of acinetobactin analogues or other members of this siderophore family, including pseudomonine and anguibactin.

Acinetobactin Isomerization Is pH-Dependent. With pure, stable pre-acinetobactin **1a** in hand, we explored a variety of analytical techniques (UV−vis, LC-MS, and NMR) to measure variable pH isomerization kinetics. Previous reports showed that pre-acinetobactin **1a** and acinetobactin **1b** have different UV−vis spectra.[24] Analysis of the changes in the optical absorption spectra (200−400 nm) of **1a** over time in phosphate buffers (pH 4.6, 7.0, and 8.8) gave time- and pH-dependent spectral changes (Figure S1A,C,E). Single-wavelength kinetic experiments of **1a** produced single-phase exponential growth curves of absorbance versus time (Figure S1B,D,F) with a clear pH-rate profile: $t_{1/2}$ pH 4.6 ≫ 7.0 > 8.0. We were able to separate isomers **1a** and **1b** by LC-MS, identify each isomer by its UV−vis spectra in the diode array (Figure S3), and monitor the isomerization over time to confirm the pH-rate relationship (Figure S2). With further optimization, these could be valuable techniques for acquisition of kinetic data in a wide range of sample matrices.

Ultimately, we found ^{1}H NMR to be most useful for accurately measuring isomerization kinetics with high reproducibility. We measured kinetics in 10% D_2O/90% H_2O and used peak integration from the diagnostic methyl doublets of pre-acinetobactin **1a** (1.42 ppm, J = 6.3 Hz) and acinetobactin **1b** (1.34 ppm, J = 6.3 Hz) to generate first-order reaction plots (Figure 2A and Figures S4−S12). A pH-rate profile for the reaction was established: $t_{1/2}$ at pH 5.5 ≫ 7.0 > 8.0. The isomerization was slow at pH 5.5 ($t_{1/2}$ = 944 ± 105 min), faster at pH 7.0 (55 ± 14 min), and fastest at pH 8.0 (18 ± 3 min) (Figure 2B), consistent with previous reports that at pH ≥8 acinetobactin **1b** forms rapidly and is stable.[16,24] However, at pH 5.5, these data suggest that pre-acinetobactin **1a** will be the

DOI: 10.1021/acsinfecdis.5b00145
ACS Infect. Dis. 2016, 2, 157−168

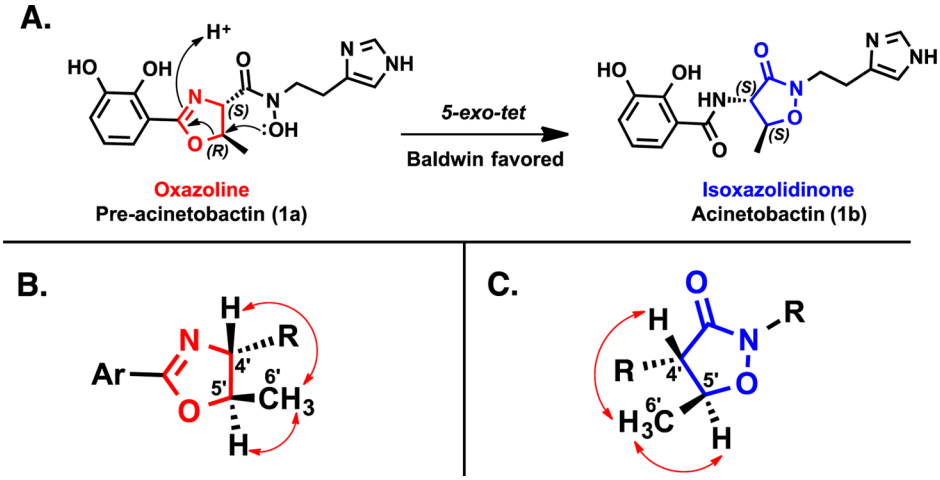

Figure 3. (A) Proposed mechanism of isomerization of pre-acinetobactin to acinetobactin. Through-space correlations on the oxazoline ring of pre-acinetobactin (B) and isoxazolidinone ring of acinetobactin (C), as observed by ROESY. Correlations between the C4′ and C5′ protons were not observed for either isomer, which supports *trans* orientation.

major isomer. Taken with knowledge that *A. baumannii* infection sites are often acidic (pH ∼5),[2,31] these data suggest that pre-acinetobactin may play an active role in iron acquisition during infection. Most *A. baumannii* pathogens grow over a wide pH range (5−8) during establishment and spread of an infection, so acinetobactin **1b** may also play a role in iron acquisition at pH >7. The isomerization kinetics suggest that pre-acinetobactin **1a** and acinetobactin **1b** will be present during *A. baumannii* infections and thus supports our hypothesis that both siderophore isomers contribute to iron acquisition in *A. baumannii* pathogens.

Kinetic isotope effects were minimized by conducting isomerization studies in 90% H_2O/10% D_2O phosphate buffer and confirmed by an experiment conducted at pH 7 in phosphate buffered D_2O (Table S1). In pure D_2O, the reaction was 2 times slower ($t_{1/2}$ = 105 ± 1 min) compared to 10% D_2O/90% H_2O ($t_{1/2}$ = 55 ± 14 min). By extrapolation, it is reasonable to assume that 10% D_2O does not affect this $t_{1/2}$ by more than the margin of error. All isomerization kinetics were performed at room temperature (27 °C). Conducting kinetic experiments at human body temperature (37 °C) gave faster kinetics, a noisier baseline, and increased experimental error. It is safe to say that the same trend in pH dependence exists at 37 °C with increased isomerization rate for all pH values.

Acinetobactin Isomerization Proceeds via Clean Inversion at C5′. To prove that reaction pH does not influence the structure and stereochemistry of acinetobactin **1b**, we analyzed synthetic acinetobactin **1b** generated at pH 5.5, 7.0, and 8.0 using C18 HPLC (Figure 2C,D), chiral HPLC (Figure 2E), CD spectrophotometry (Figure S13), and high-resolution MS−MS (Figures S14−S16). Acinetobactin **1b** isolated from isomerization of pre-acinetobactin **1a** at pH 5.5, 7.0, and 8.0 gave identical retention times and UV−vis spectra when analyzed by C18 HPLC individually and as a mixture (Figure 2C). A mixture of acinetobactin **1b** samples generated at pH 5.5, 7.0, and 8.0 showed identical retention times and UV−vis spectra when analyzed by C18 HPLC compared to a natural analytical acinetobactin **1b** standard purified from *A. baumannii* (Figure 2D). High-resolution MS−MS analysis of synthetic and natural acinetobactin samples supported the matching identity of these samples through confirmation of molecular formula (Figures S14−S16) and characteristic mass fragmentation patterns (Schemes S3−S6). To assess the stereochemical purity of the various samples, chiral HPLC and CD spectrophotometry were performed. The natural and synthetic acinetobactin **1b** samples generated at all pH values showed identical retention times on chiral HPLC (Figure 2E) and identical CD spectra (Figure S13). These data suggest that the synthetic acinetobactin samples match the natural samples in both enantiomeric and diastereomeric identity and purity and that the pH does not influence stereochemical outcome of the isomerization reaction.

The acinetobactin isomerization reaction was slow at pH 5.5 and fast at pH >7 (Figure 2B), consistent with a proposed mechanism where the hydroxamate of **1a** acts as nucleophile at C5′ of the oxazoline. If the hydroxamate attacks the oxazoline C5′ in S_N2 manner, inducing a Baldwin-favored, 5-*exo-tet* cyclization,[33] the result would be clean stereochemical inversion at C5′ (*R* to *S*) while maintaining stereochemistry at C4′ (*S*) (Figure 3A). If this type of mechanism were at play, then both the pre-acinetobactin **1a** oxazoline and the acinetobactin **1b** isoxazolidinone heterocycles would have a *trans* orientation of the C4′ and C5′ stereogenic centers. Indeed, ROESY 2D NMR analysis of pre-acinetobactin (Figure 3B and Table S2) and acinetobactin (Figure 3C and Table S3) showed strong signals for through-space interactions between C4′−C6′ protons and C5′−C6′ protons for both **1a** and **1b** structures. There were no observable ROESY correlations for C4′−C5′ protons in both acinetobactin isomers, which is consistent with a *trans* orientation of C4′ and C5′ stereocenters in the oxazoline and isoxazolidinone heterocycles of pre-acinetobactin **1a** and acinetobactin **1b**, respectively. We used enantiomerically pure L-threonine in our synthesis of pre-acinetobactin **1a** and acinetobactin **1b**, which allows assignment of the stereochemistry at C4′ and C5′ for each isomer (pre-acinetobactin **1a**, C4′ (*S*) and C5′ (*R*); acinetobactin **1b**, C4′ (*S*) and C5′ (*S*)). Collectively, our chiral HPLC, multidimensional NMR, high-resolution MS−MS, and CD studies indicate high diastereo- and enantiomeric purity (>95%) and equivalence between the synthetic acinetobactin **1b** samples generated at pH 5.5, 7.0, and 8.0 and authentic acinetobactin isolated from *A. baumannii* ATCC 17978. Considering the general pK_a of a hydroxamic acid (∼9),[34] the pH-rate profile for the pre-acinetobactin isomerization (Figure 2B; pH-rate profile: $t_{1/2}$ pH

DOI: 10.1021/acsinfecdis.5b00145
ACS Infect. Dis. 2016, 2, 157−168

5.5 ≫ 7.0 > 8.0) is consistent with deprotonation of the hydroxamic acid at neutral or higher pH values, which increases the rate of nucleophilic attack on C5′. A 5-*exo-tet* cyclization mechanism where the hydroxamate attacks C5′ in S_N2 manner accounts for the stereochemical outcome of the reaction and is consistent with the measured first-order pH-rate profile. There are likely subtle electronic factors and proton transfer events that contribute to the mechanism and kinetics of pre-acinetobactin isomerization that require further study.

Acinetobactin and Pre-acinetobactin Form Unique, Stable Complexes with Fe(III). Pre-acinetobactin isomerization kinetics suggest that the oxazoline isomer **1a** is stable at pH 5.5 ($t_{1/2}$ = 944 min) and relatively unstable at pH 7.0 ($t_{1/2}$ = 55 min) and 8.8 ($t_{1/2}$ = 18 min) (Figure 2B). We propose that pre-acinetobactin **1a** will be stable at acidic sites of *A. baumannii* infection and acinetobactin **1b** will be stable at neutral to basic sites of infection. If both isomers are to be considered biologically relevant siderophores over this pH range, it is critical to investigate the ability of each isomer to form stable complexes with iron(III). We prepared pre-acinetobactin− and acinetobactin−iron(III) complexes, **1a-Fe(III)** and **1b-Fe(III)**, respectively, by treating methanolic solutions of the iron-free siderophores, **1a** and **1b**, with 1.1 equiv of tris(acetylacetonato) iron(III) (Scheme 1). Upon addition of tris(acetylacetonato) iron(III), the reactions instantly turned dark purple/black, indicating that a metal complex was formed for both isomers. Both the pre-acinetobactin−iron(III) complex **1a-Fe(III)** and the acinetobactin−iron(III) complex **1b-Fe(III)** are soluble in methanol and aqueous buffers upon sonication.

Each siderophore−iron(III) complex gives a unique UV−vis absorbance spectrum (Figure 4). The pre-acinetobactin−iron(III) complex **1a-Fe(III)** is clear and magenta in color with a broad peak at 515 nm. The acinetobactin−iron(III) complex **1b-Fe(III)** is clear and purple with a broad peak at 570 nm. Titrating NMR quantified solutions of the apo-siderophores with tris(acetylacetonato) iron(III) indicated a ligand/metal ratio of ∼2:1 (Figure S20). Extinction coefficients were calculated for the apo-siderophores and iron complexes (assuming a 2:1 siderophore/Fe(III) stoichiometry).

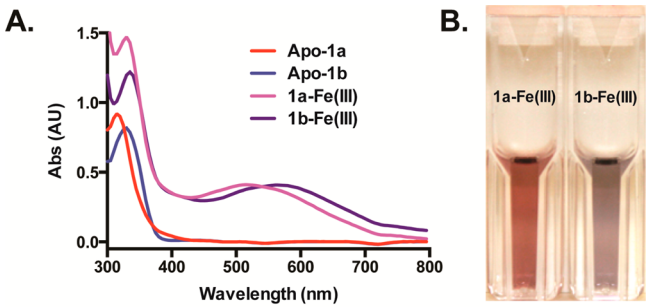

Figure 4. (A) UV−vis absorption spectra for 290 mM apo-pre-acinetobactin **1a**, 256 mM apo-acinetobactin **1b**, pre-acinetobactin−iron(III) **1a-Fe(III)**, and acinetobactin−Fe(III) **1b-Fe(III)** (apo-siderophores fully titrated with Fe^{3+}) (10 mM HEPES, pH 7.4). (B) Solutions of pre-acinetobactin−Fe(III) (left) and acinetobactin−Fe(III) (right) (10 mM HEPES, pH 7.4).

The pre-acinetobactin−iron(III) complex **1a-Fe(III)** was stable in phosphate buffered M9 media at pH 5.7, 6.5, and 7.5 at room temperature for >3 weeks with no measurable change in the UV−vis spectrum. Iron-free pre-acinetobactin **1a** isomerizes rapidly at pH 7.5 ($t_{1/2}$ < 55 min), but the iron(III) complex **1a-Fe(III)** does not, which suggests that the metal protects pre-acinetobactin from isomerizing. This is consistent with the hydroxamate N−O making a strong interaction with the iron(III) center in a conformation that does not favor the 5-*exo-tet* cyclization (Figure 3A). The acinetobactin−iron(III) complex **1b-Fe(III)** was stable in phosphate buffered M9 media at pH 6.5 and 7.5 at room temperature for >3 weeks but was unstable at pH 5.7. Addition of the purple acinetobactin−Fe(III) complex to pH 5.7 M9 media resulted in a clear, colorless solution, suggesting instability of the complex under these conditions. This is consistent with a catecholate participating as a bidentate ligand for iron(III) compared to the phenylateoxazoline bidentate ligand in pre-acinetobactin. Protonation of the more basic catecholate at acidic pH will block its ability to chelate Fe(III). A similar dual mode of catecholate versus phenolateoxazoline is observed for the siderophore vibriobactin from *Vibrio cholerae*, where swapping coordination modes influences siderocalin binding.[35] We observed a blue spectral shift when comparing the **1a-Fe(III)** complex (λ = 515 nm) to the **1b-Fe(III)** complex (λ = 570 nm). Such spectral shifts are observed for other strong-field catechol ligands such as bis-catecholate−Fe(III) (λ = 575 nm) and tris-catecholate enterobactin−Fe(III) (λ = 498 nm).[36] In the observed case, such a spectral shift indicates unique ligand to metal coordination modes for the **1a-Fe(III)** and **1b-Fe(III)** complexes that might be explained when considering catecholate versus phenolateoxazoline chelation modes. The stability of the pre-acinetobactin−Fe(III) complex at pH 5.7, and corresponding instability of the acinetobactin−Fe(III) complex at pH 5.7, supports our hypothesis that pre-acinetobactin acts as a siderophore for *A. baumannii* at acidic infection sites and acinetobactin serves as a siderophore under more basic conditions. Improved knowledge of coordination chemistry in the pre-acinetobactin and acinetobactin family of siderophores is important for understanding iron transport in *A. baumannii* and other pathogens.[37]

Both Acinetobactin Isomers Serve as pH-Dependent Iron Sources for *A. baumannii*. The capacity to biosynthesize and transport acinetobactin has been validated in several studies using *A. baumannii* wild-type and knockout strains both in vitro and in vivo.[19] Acinetobactin is an important virulence factor for pathogenic *A. baumannii*. All genome sequenced clinical isolates possess a functional acinetobactin gene cluster with biosynthesis and utilization genes (>50 in total; only *A. baumannii* AYE clinical isolate is believed to not produce acinetobactin, although it does possess the biosynthetic gene cluster with a functional mutation in *entA*[18]).[11] However, there are no reports clarifying which siderophore isomer, pre-acinetobactin **1a** or acinetobactin **1b**, or both, is biologically relevant.

We investigated pre-acinetobactin− and acinetobactin−Fe(III) complexes as iron sources for *A. baumannii* by performing feeding studies in defined M9 media buffered at pH 5.7, 6.5, and 7.5. As described in the previous section, pre-acinetobactin−Fe(III) complex **1a-Fe(III)** is stable and does not undergo isomerization at pH 5.7, 6.5, and 7.5, which allowed for testing the growth-promoting activity of this isomer without substantial conversion to acinetobactin−Fe(III) complex **1b-Fe(III)**. *Acinetobacter baumannii* ATCC 17978 grows well in the buffered M9 media at all pH values. For each buffered M9 media, we initially performed growth studies with increasing amounts of 2,2′-dipyridyl (DIP) to make the growth media iron replete enough to entirely halt the growth of *A.*

DOI: 10.1021/acsinfecdis.5b00145
ACS Infect. Dis. 2016, 2, 157−168

baumannii ATCC 17978 (200 μM for pH 5.7, 250 μM for pH 6.5, and 250 μM for pH 7.5; Figure S35, black control growth curves).[22] We next performed the same growth studies where cultures were supplemented with a gradient of either pre-acinetobactin−Fe(III), **1a-Fe(III)**, or acinetobactin−Fe(III), **1b-Fe(III)**, at concentrations spanning 50−0.84 μM (Figure S35). Growth curves were generated by measuring optical density at 700 nm (OD_{700}) with a final reading taken after 45 h (Figure 5).

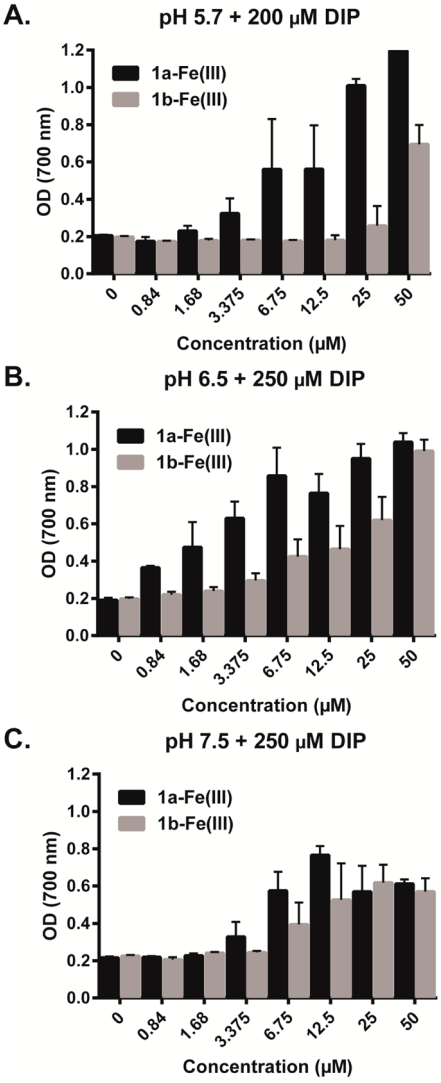

Figure 5. Growth as measured by OD_{700} (*y*-axis) of *A. baumannii* ATCC 17978 microplate cultures in buffered M9 media at pH 5.7 with 200 μM DIP (A), 6.5 with 250 μM DIP (B), and 7.5 with 250 μM DIP (C) at 45 h supplemented with a 0−50 μM (*x*-axis) gradient of pre-acinetobactin−Fe(III), **1a-Fe(III)**, or acinetobactin−Fe(III), **1b-Fe(III)**.

Comparison of full growth curves (Figure S35) and the 45 h OD_{700} reading (Figure 5A−C) show that both pre-acinetobactin−Fe(III) and acinetobactin−Fe(III) promote the growth of *A. baumannii* ATCC 17978 under iron-deficient conditions at all pH values in a dose-dependent manner. At pH 5.7, pre-acinetobactin−Fe(III) boosted growth starting at 1.68 μM, while acinetobactin−Fe(III) did not promote growth substantially relative to the control until reaching 25−50 μM. At pH 6.5, pre-acinetobactin−Fe(III) and acinetobactin−Fe(III) both promoted *A. baumannii* growth starting at 0.84 μM, with more pronounced growth promotion from pre-acinetobactin−Fe(III) from 0.84 to 25 μM. At pH 7.5, the growth promotion from both isomers is comparable starting at 3.375 μM. These data support that both siderophore isomers, pre-acinetobactin−Fe(III) and acinetobactin−Fe(III), are capable of serving as iron sources for *A. baumannii* ATCC 17978. Furthermore, there is a pH preference for each siderophore isomer. Pre-acinetobactin−Fe(III) is more competent to promote *A. baumannii* growth under acidic conditions (pH 5.7). At pH 5.7, the acinetobactin−Fe(III) complex was found to be unstable, as discussed previously, which is consistent with the observation that it serves poorly as an iron source at pH 5.7 compared to pre-acinetobaction−Fe(III). Collectively, these growth promotion studies (Figure 5) are consistent with pre-acinetobactin isomerization kinetics (Figure 2B) and support a model where pre-acinetobactin **1a** serves as siderophore for *A. baumannii* at acidic pH and isomerizes to acinetobactin **1b** under neutral to basic conditions to continue serving as a competent siderophore. These studies also suggest that *A. baumannii* ATCC 17978 possesses uptake machinery for internalizing both pre-acinetobactin− and acinetobactin−Fe-(III) complexes.

Pre-acinetobactin and Acinetobactin Use the Same Outer-Membrane Transport Protein. We performed growth promotion studies using siderophore transport and biosynthesis mutants to test if pre-acinetobactin **1a-Fe(III)** and acinetobactin **1b-Fe(III)** utilize the same membrane transport system in *A. baumannii* pathogens (Figures 6 and S36). Actis and co-workers prepared and characterized gene insertion mutants of the clinical isolate *A. baumannii* ATCC 19606, a producer of acinetobactin, with functionally disabled outer membrane receptor *bauA* (mutant **t6**), inner membrane ABC transporter *bauD* (mutant **t7**), or biosynthetic oxazoline cyclization enzyme *basD* (mutant **s1**).[22] As expected, we found that both **1a-Fe(III)** and **1b-Fe(III)** promoted the growth of wild-type and **s1** biosynthesis mutant *A. baumannii* strains, which have fully functional transport systems (Figure 6). Also as expected, the **t6** outer membrane receptor mutant was unable to utilize either siderophore isomer as a source of iron, suggesting that both siderophore−iron(III) complexes rely on the same outer membrane receptor, bauA, for entry into the periplasmic space of the cell. Surprisingly, the **t7** inner membrane ATP-dependent transporter *bauD* mutant was still able to utilize **1b-Fe(III)** (Figure 6B) and to a lesser extent **1a-Fe(III)** (Figure 6A) as a source of iron. Since *A. baumannii* ATCC 19606 also produces the fimsbactin and baumannoferrin siderophores, it is possible that certain siderophore utilization proteins, such as the inner membrane ABC transporters and periplasmic siderophore binding proteins,[34] can be shared between various siderophore systems, leaving the outer membrane receptors as the gatekeepers for selective siderophore transport.

***A. baumannii* Excretes Pre-acinetobactin to the Extracellular Space.** In order for pre-acinetobactin and acinetobactin to act as siderophores, pre-acinetobactin must be excreted by *A. baumannii* to the extracellular space, where it can isomerize to acinetobactin or acinetobactin might also be excreted after intracellular isomerization. Walsh and co-workers detected pre-acinetobaction production directly from in vitro reconstitution of the pseudomonine NRPS assembly line (PmsEDG).[24] Under these conditions (pH 8.0), enzymatically

DOI: 10.1021/acsinfecdis.5b00145
ACS Infect. Dis. 2016, 2, 157−168

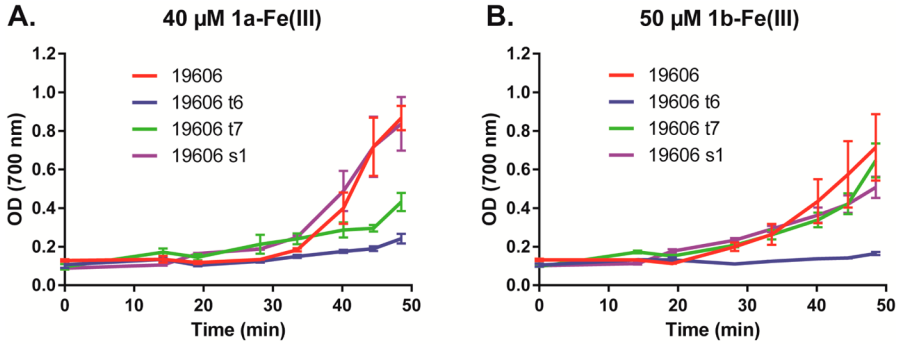

Figure 6. Growth of *A. baumannii* ATCC 19606 and mutants **t6**, **t7**, and **s1** in M9 minimal media pH 6.5 + 250 μM DIP. (A) Media supplemented with 40 μM **1a-Fe(III)**. (B) Media supplemented with 50 μM **1b-Fe(III)**.

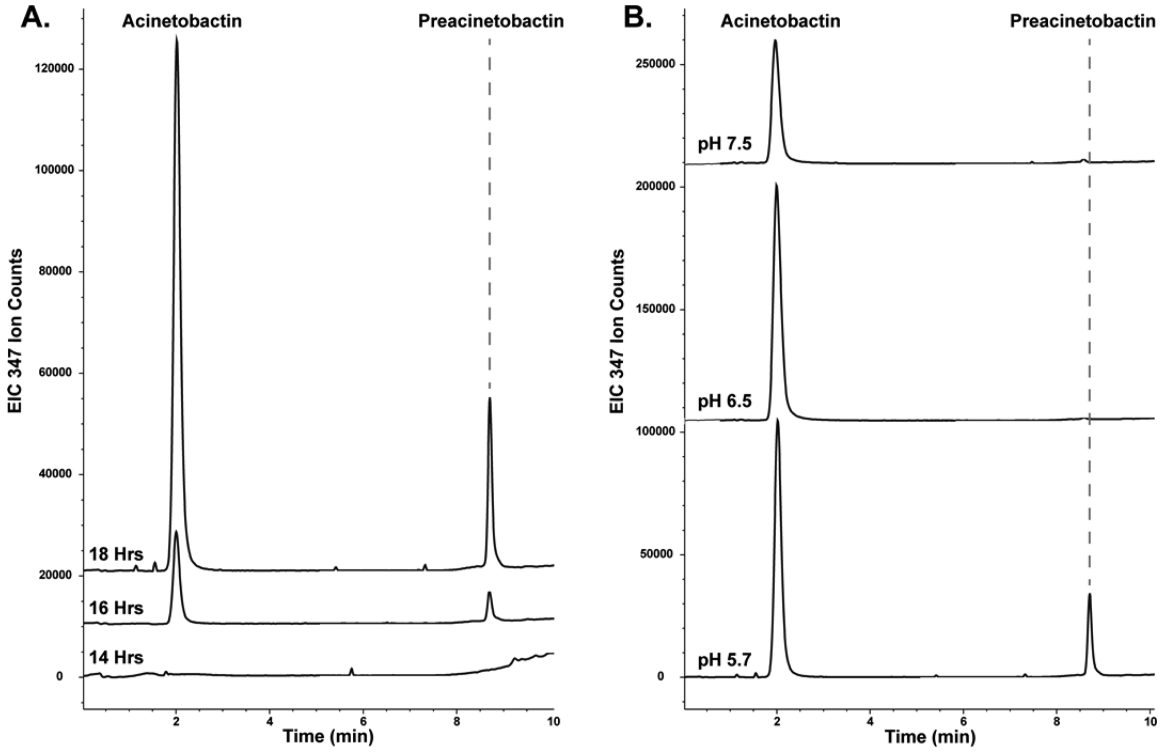

Figure 7. Detection of pre-acinetobactin and acinetobactin in *A. baumannii* ATCC 17978 culture supernatants by LC-MS via extracted-ion chromatograms of [M + H] = 347. Retention times are normalized to acinetobactin standards and confirmed by UV−vis analysis. (A) Chromatograms from single culture grown in M9 media at pH 5.7 and measured at set time points. (B) Chromatograms from cultures grown in M9 media at pH 5.7, 6.5, and 7.5, taken after 18 h of growth. Peak heights do not represent absolute concentration.

produced pre-acinetobactin rapidly isomerized to acinetobactin as monitored by HPLC. There are no reports of pre-acinetobactin detected in the extracellular space of growing *A. baumannii* cultures. By growing *A. baumannii* ATCC 17978 in M9 media buffered to pH 5.7, we were able to detect pre-acinetobactin and acinetobactin in the culture supernatant using LC-MS (Figure 7A). As expected, based on isomerization kinetics reported in this study (Figure 2B), no pre-acinetobactin was detected in cultures grown at pH 6.5 and 7.5 (Figure 7B). Detection of pre-acinetobactin and acinetobactin in *A. baumannii* culture supernatants implies that *A. baumannii* possesses efflux machinery capable of exporting pre-acinetobactin. Acinetobactin might also be exported after intracellular isomerization, or it could isomerize in the extracellular space following pre-acinetobactin efflux. This model accounts for use of both siderophore isomers, in an adaptable manner, for iron acquisition over a wide pH range and diverse infection environments.

OUTLOOK AND CONCLUSIONS

Many highly virulent bacterial pathogens such as uropathogenic *Escherichia coli*, *Pseudomonas aeruginosa*, and *Vibrio cholerae* produce a cocktail of siderophores for iron acquisition during host invasion.[34,38,39] Advantages of siderophore combinations might include tuning iron acquisition toward specific tissues and iron sources (i.e., different infection pH or sequestration from host lactoferrin or transferrin repositories[40]), evasion of the human immune system (i.e., sequestration by siderocalin), chemical signaling (i.e., quorum sensing and biofilm formation), or metal detoxification (i.e., copper detox by yersiniabactin).[15,37,41] Pathogenic *A. baumannii* produce multiple sideorphores, typically the fimsbactins,[17] baumannofer-

DOI: 10.1021/acsinfecdis.5b00145
ACS Infect. Dis. 2016, 2, 157−168

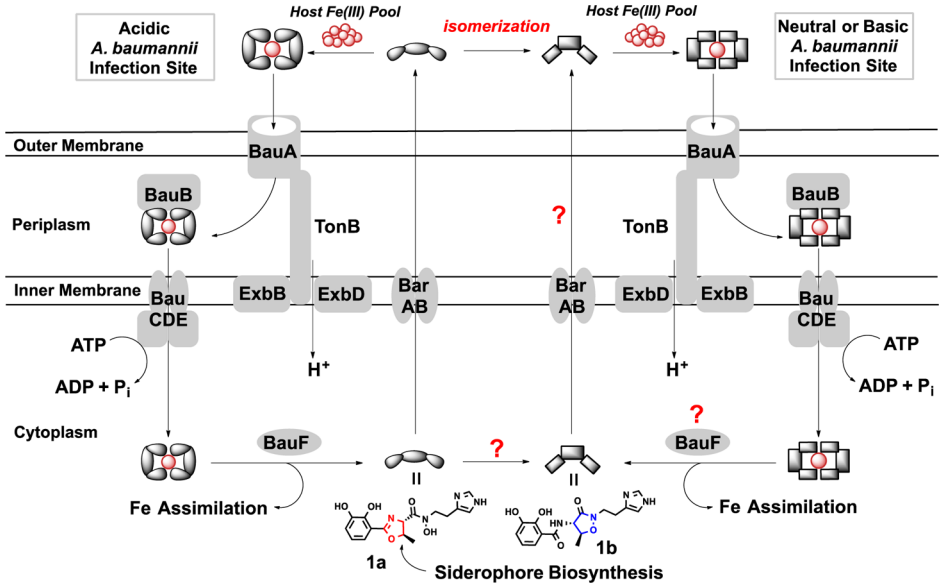

Figure 8. Proposed model of pH-triggered siderophore swapping in pathogenic *A. baumannii*. Pre-acinetobactin, **1a**, is biosynthesized in the cytoplasm and excreted via efflux pump BarAB. Under acidic infection conditions, pre-acinetobactin serves as the siderophore to sequester iron(III) and gain access into the cell via the BauA outer membrane receptor and the TonB/ExbB/ExbD complex, BauB periplasmic siderophore binding protein, and BauCDE inner membrane transporter. Once in the cytoplasm, BauF, a predicted hydrolase, assists in assimilation of iron. Alternatively, if the infection site is neutral or basic, the excreted pre-acinetobactin **1a** will rapidly isomerize to acinetobactin **1b**, which sequesters iron(III) and gains entry into the cell using the same pathway described for **1a**. Our results clearly show that the isomerization can happen in the extracellular space (Figure 7), but it is also possible that the isomerization takes place in the cytoplasm and both **1a** and **1b** are directly effluxed. The intracellular fate of both siderophore isomers **1a** and **1b** after influx of the siderophore−iron(III) complex is currently unknown.

rins,[18] and acinetobactin.[16] Acinetobactin, the focus of this work, is the best studied of the *A. baumannii* siderophores, and it is a validated, highly conserved virulence factor.[19]

The fimsbactins[17] are mixed ligand, bis-catecholate monohydroxamate siderophores that are reminiscent of enterobactin, salmochelin, vibriobactin, and petrobactin catechol siderophores that act as high-affinity iron(III) chelators (enterobactin $K_{Fe} \sim 10^{49}$) and play important roles as siderocalin binding substrates or stealth siderophores for evasion of the host immune system.[34,36] Baumannoferrin[18] is also a mixed ligand bis-α-hydroxy carboxylate monohydroxamate siderophore with a C10-acyl lipid tail. Baumannoferrin resembles another siderophore, acinetoferrin,[42] from nonpathogenic, environmental *A. hemolyticus* ATCC 17906T, which has been shown to be membrane associated.[43] Baumannoferrin might serve as a hydrophobic, membrane-associated siderophore that does not diffuse far from the *A. baumannii* cell surface, or it might enhance in iron sequestration in more hydrophobic infection environments.

Although *A. baumannii* pathogens only produce three siderophores, we have shown that both isomers of acinetobactin, oxazoline-containing pre-acinetobactin **1a** and isooxazolidinone-containing acinetobactin **1b**, likely contribute to iron acquisition, making an overall net effective total of four siderophores. Additionally, *A. baumannii* pathogens are known to express receptor/transport proteins for xenosiderophores, further expanding capacity for siderophore usage.[44] Acinetobactin isomerization appears to be an adaptation strategy for *A. baumannii* to expand the pH window for iron acquisition. Siderophores, as iron(III) chelating ligands, are in constant competition for binding to metals or protons.[34] The fimsbactins will likely be unable to form high-affinity iron(III) complexes under acidic pH, which is required for successful iron(III) sequestration because the bis-catecholate ligands will be protonated ($pK_a \sim 9.2, 13.0$). Baumannoferrin will likely be able to bind iron(III) under acidic conditions because the α-hydroxy carboxylate ($pK_a \sim 3.0$) and hydroxamate ($pK_a \sim 9.0$) ligands are more deprotonated and therefore more effective than catecholates at acidic pH. However, it is unknown if baumannoferrin will be diffuse or membrane-bound during the infection. This leaves pre-acinetobactin as a viable siderophore to service iron acquisition at acidic infection sites. Pre-acinetobactin is stable at acidic pH ($t_{1/2}$ = 944 min at pH 5.5) and capable of iron(III) chelation from pH 5.7 to 7.5. Acinetobactin is rapidly formed via pre-acinetobactin spontaneous isomerization at pH >7 ($t_{1/2}$ < 55 min) and is capable of iron(III) chelation at pH >6.5. Pre-acinetobactin is excreted by *A. baumannii*, and the external pH ultimately determines which isomer will serve as siderophore. Acinetobactin isomerization is a flexible siderophore swapping strategy for *A. baumannii* to adapt to its environment and maximize its capacity for iron acquisition (Figure 8).

Other siderophores, including vibriobactin[35] from *V. cholerae* and the staphyloferrins A and B,[45] produced by MRSA as a virulence factor, are capable of non-enzymatic ligand isomerizations and metal chelation isomerizations. Perhaps this strategy has been evolved broadly among siderophore classes to enable more flexibility in metal chelation and environmental adaptability to ultimately enhance microbial iron acquisition. Acinetobactin isomerization and coordination chemistry require firm understanding in order to properly frame biological findings. Siderophore pathways are attractive targets for novel antibacterial agents (i.e., antibiotic drug delivery[46,47]), antivirulence therapeutics (i.e., siderophore biosynthesis inhibitors[10] and gallium quenching[48]), vaccine development,[49] and infection diagnostics (i.e., siderophore imaging[50] and diagnostic agents[51]).[52] Our work establishes that pre-acinetobactin and acinetobactin are both biologically relevant siderophores for

DOI: 10.1021/acsinfecdis.5b00145
ACS Infect. Dis. 2016, 2, 157−168

pathogenic *A. baumannii* and directs future studies in pathogenesis and siderophore-based therapeutics/diagnostics to consider both isomers of this siderophore family.

MATERIALS AND METHODS

Strains, Materials, and Instrumentation. Growth studies were conducted using *Acinetobacter baumannii* ATCC 17978, 19606, and 19606 derivatives **t6** (bauA::EZ::TN<R6Kcori/KAN-2>), **t7** (bauD::EZ::TN<R6Kcori/KAN-2>), and **s1** (basD::aph) provided by Dr. Luis Actis. Acinetobactin production was conducted using *Acinetobacter baumannii* ATCC 17978. Glycerol stocks of *A. baumannii* were made from cells grown in LB media and stored at −80 °C. Precultures and 96-well plate *A. baumannii* growth assays were performed in pH-adjusted, filter-sterilized M9 minimal media (see Supporting Information for recipe). Samples for HPLC and LC-MS were prepared in 0.45 μm PTFE Mini-UniPrep vials from Agilent. All pH measurements were recorded using an Orion Star A111 pH meter and a PerpHecT ROSS micro combination pH electrode from Thermo Scientific. Analytical HPLC was performed using Beckman Coulter SYSTEM GOLD 126 solvent module, 508 autosampler, and 168 detector. A Luna 5 μm C18(2) 100A column, 250 × 4.6 mm with guard column, was used for achiral separations, and a Lux 5u cellulose-1 column, 100 × 4.6 mm, was used for chiral separations, both from Phenomenex. All preparatory HPLC was performed using a Beckman Coulter SYSTEM GOLD 127P solvent module and 168 detector with a Phenomenex Luna 10u C18(2) 100A column, 250 × 21.20 mm, 10 μm with guard column. Analytical and prep HPLC were performed with mobile phases of 0.1% trifluoroacetic acid in (A) water and (B) acetonitrile, and data were processed using 32 Karat software, version 7.0. All LC-MS was performed on an Agilent 6130 quadrupole LC-MS with G1313 autosampler, G1315 diode array detector, and 1200 series solvent module. A Phenomenex Gemini C18 column, 50 × 2 mm, 5 μm with guard column was used for all LC-MS separations. LC-MS mobile phases were 0.1% formic acid in (A) water and (B) acetonitrile, and data were processed using G2710 ChemStation software. NMR was performed on Varian Unity Plus-300 MHz and Varian Unity Inova-500 MHz instruments. UV−vis spectroscopy was performed on a Cary 50 fit with an autosampler and water Peltier thermostat system using 1 cm quartz cuvettes. CD spectroscopy was performed on a Jasco-J715 spectropolarimeter in a 0.1 cm cuvette. Bacterial growth studies were performed using polystyrene 96-well plates with lids sealed using parafilm, and OD_{700} measurements were taken on a Molecular Devices SpectraMax Plus 384 plate reader.

Synthesis of Acinetobactin and Pre-acinetobactin. *Pre-acinetobactin TFA Salt (**1a**).* Benzyl pre-acinetobactin **12** was synthesized as described previously[32] (Scheme S2) and purified by prep HPLC as the TFA salt using a gradient of 5% B to 95% B over 20 min. Pure **12** TFA salt was stirred in methanol with ∼1:10 mass equivalent of 10% Pd/C under a hydrogen atmosphere. Once complete as judged by LC-MS (1 h), the mixture was flushed with argon, filtered, and concentrated by rotary evaporation. Solutions of **1a** TFA salt in deuterated methanol were quantified by ^{1}H NMR using an acetonitrile internal standard. This material was >95% pure and used without further purification: ^{1}H NMR (500 MHz, $(CD_3)_2SO$) δ (ppm) 10.40 (br s, 1 H), 8.97 (s, 1 H), 8.49 (br s, 1 H), 7.43 (s, 1 H), 7.04 (dd, J = 1.6, 7.8 Hz, 1 H), 6.96 (dd, J = 1.6, 7.8 Hz, 1 H), 6.74−6.70 (m, 1 H), 5.00 (d, J = 6.3 Hz, 1 H), 4.80 (td, J = 6.2, 11.9 Hz, 1 H), 4.00−3.72 (m, 2 H), 3.05−2.90 (m, 2 H), 1.42 (d, J = 6.3 Hz, 3 H); ^{13}C NMR (500 MHz, $(CD_3)_2SO$) δ (ppm) 21.7, 23.0, 47.0, 71.5, 80.1, 117.8, 119.2, 120.0, 120.8, 131.7, 135.4, 147.0, 150.0, 167.3, 170.9; HRMS (ESI) calcd mass for [M + H] ($C_{16}H_{19}O_5N_4^+$) m/z 347.1350, found 347.1355; molar extinction coefficient (10 mM HEPES buffer, pH 7.4) 3147 M^{-1} cm^{-1} at 315 nm. See Supporting Information for MS−MS fragmentation and tabulated 2D NMR data.

*Acinetobactin TFA Salt (**1b**).* Pre-acinetobactin **1a** TFA salt was dissolved in 0.2 M phosphate buffer (pH 5.5−8) and left overnight. The product was purified by preparatory HPLC using a gradient of 5% B to 95% B over 20 min. Solutions in D_2O were quantified by ^{1}H NMR using an acetonitrile internal standard: ^{1}H NMR (500 MHz, $(CD_3)_2SO$) δ (ppm) 9.33 (br s, 1 H), 9.05 (d, J = 8.6 Hz, 1 H), 8.98 (s, 1 H), 7.51 (s, 1 H), 7.24 (d, J = 7.0 Hz, 1 H), 6.93 (d, J = 7.8 Hz, 1 H), 6.75−6.63 (m, 1 H), 4.61 (dd, J = 8.2, 10.6 Hz, 1 H), 4.46−4.34 (m, 1 H), 3.81 (t, J = 6.7 Hz, 2 H), 3.04−2.86 (m, 2 H), 1.34 (d, J = 6.3 Hz, 3 H); ^{13}C NMR (500 MHz, $(CD_3)_2SO$) δ (ppm) 18.0, 23.3, 45.2, 58.4, 79.0, 116.3, 118.2, 119.0, 119.7, 120.7, 131.3, 135.4, 147.6, 150.5, 169.0, 171.0; HRMS (ESI) calcd mass for [M + H] ($C_{16}H_{19}O_5N_4^+$) m/z 347.1350, found 347.1350; molar extinction coefficient (10 mM HEPES buffer, pH 7.4) 3176 M^{-1} cm^{-1} at 330 nm. See Supporting Information for MS−MS fragmentation and tabulated 2D NMR data.

*Pre-acinetobactin−Fe(III) Complex (**1a-Fe(III)**).* Pre-acinetobactin **1a** was dissolved in methanol and treated with 1.1 equiv of tris(acetylacetonato) iron(III). The solution was concentrated by rotary evaporation, and the residue was triturated with diethyl ether. Product **1a-Fe(III)** was isolated in >95% purity as a black powder. HRMS (ESI) calcd mass for [M + Fe − 2H] ($C_{16}H_{16}FeO_5N_4^+$) m/z 400.0465, found 400.0451; molar extinction coefficient (10 mM HEPES buffer, pH 7.4) 2829 M^{-1} cm^{-1} at 515 nm and 1269 M^{-1} cm^{-1} at 650 nm.

*Acinetobactin−Fe(III) Complex (**1b-Fe(III)**).* Acinetobactin−iron complex **1b-Fe(III)** was isolated as a black powder following an analogous procedure described for **1a-Fe(III)**. HRMS (ESI) calcd mass for [M + Fe − 2H] ($C_{16}H_{16}FeO_5N_4^+$) m/z 400.0476, found 400.0447; molar extinction coefficient (10 mM HEPES buffer, pH 7.4) 3171 M^{-1} cm^{-1} at 570 nm and 2165 M^{-1} cm^{-1} at 650 nm.

Isolation and Purification of Acinetobactin from *A. baumannii* Cultures. A 5 mL preculture of *A. baumannii* ATCC 17978 in M9 minimal media was grown overnight at 37 °C. Preculture (100 μL) was added to 1 L of sterile M9 in a 3 L shaker flask and incubated at 37 °C with shaking (225 rpm) for 48 h. Cells were pelleted (5000 rpm, 20 min), and the supernatant was adjusted to pH 6 with saturated citric acid. Resin (XAD-7HP, 25 g) was added, and the mixture was shaken at 125 rpm for 2 h. The mixture was filtered, and the resin was washed with DI H_2O (3 × 500 mL). The resin was treated with 200 mL of MeOH, shaken at 125 rpm for 30 min, filtered, and washed with 900 mL of MeOH. The MeOH was concentrated by rotary evaporation and purified by preparatory HPLC using a gradient of 5% B to 95% B over 20 min to yield 50 mg of pure acinetobactin, **1b**, TFA salt. All characterization data matched synthetic acinetobactin.[16]

Acinetobactin Isomerization Kinetic Studies. Pre-acinetobactin **1a** isomerization to actinetobactin **1b** kinetics were measured using ^{1}H NMR spectroscopy in three independent trials for each pH value (5.5, 7.0, and 8.0). Pre-

DOI: 10.1021/acsinfecdis.5b00145
ACS Infect. Dis. 2016, 2, 157−168

acinetobactin (1 mg) was dissolved in 0.6 mL of buffered (0.2 M, pH 5.5, 7.0, and 8.0) 10% D_2O/90% H_2O in an NMR tube, and ^1H NMR spectra (500 MHz, 27 °C) were collected every 40 s to 10 min. Peak integrations over time were used to generate first-order reaction plots and calculate half-lives (Supporting Information, Figures S4−S12).

***A. baumannii* Growth Studies in Minimal Media.** *Acinetobacter baumannii* ATCC 17978 preculture was grown overnight at 37 °C in M9 media. A McFarland 0.5 standard was prepared in sterile 0.9% aqueous sodium chloride solution.[53] M9 medium (29.8 mL) was inoculated with 0.2 mL of the 0.5 McFarland standard, making a 1×10^5 cfu/mL inoculum. All growth studies were performed in triplicate in 96-well plates.

Total inhibitory concentrations of 2,2′-dipyridyl (DIP) were determined for buffered M9 media (pH 5.7, 6.5 and 7.5) using 200 μL total volume per well of inoculated M9 media at varying DIP concentrations (200, 100, 50, 25 μM). Each well was filled with 100 μL of sterile M9 media. Next, 100 μL of a filter sterilized 4× solution of DIP (800 μM) in M9 media was added to the first well of each row. Two-fold serial dilutions were performed across each row, providing a gradient of 200−25 μM DIP. Inoculated M9 medium (100 μL) was added to each well, and the plate was incubated at 37 °C shaking at 150 rpm. The OD_{700} of each well was collected every hour for 48 h.

To determine restorative concentrations of supplemented siderophore−iron(III) complexes in the presence of total inhibitory DIP, growth assays were performed using 200 μL total volume per well of inoculated M9 media (pH 5.7 + 200 μM DIP, pH 6.5 + 250 μM DIP, pH 7.5 + 250 μM DIP) with gradient concentrations of **1a-Fe(III)** and **1b-Fe(III)**. Each well was filled with 100 μL of sterile, noninoculated M9 media + DIP. The first well of each row was filled with 100 μL of a filter sterilized 4× solution of **1a-Fe(III)** (800 μM) in M9 media + DIP or 100 μL of a filter sterilized 4× solution of **1b-Fe(III)** (800 μM) in M9 media + DIP. Two-fold serial dilutions were performed across each row providing a 200−0.1 μM gradient of **1a-Fe(III)** or **1b-Fe(III)**. Inoculated M9 media + DIP (100 μL) were added to each well. A control plate was prepared for each pH, with no siderophore supplement, using 100 μL sterile M9 media + DIP and 100 μL inoculated M9 media + DIP in each well (200 μL final volume). The plates were incubated at 37 °C with shaking at 150 rpm. The OD_{700} of each well was collected over 48 h.

Growth studies on *A. baumannii* ATCC 19606 and associated derivatives were conducted in M9 minimal media pH 6.5 + 250 μM DIP. Each well was filled with 100 μL of either 2× **1a-Fe(III)** or 2× **1b-Fe(III)** dissolved in M9 media + DIP to give a concentration gradient from left to right (240, 220, 200, 180...20 μM). Inoculated M9 media + DIP (100 μL) was added to each well, and plates were incubated at 37 °C with shaking at 150 rpm. The OD_{700} of each well was collected over 48 h.

Detection of Acinetobactin Isomers in *A. baumannii* Cultures. Overnight cultures of *A. baumannii* ATCC 17978 in LB broth were used to prepare a 0.5 McFarland standard in sterile saline as inoculum (100 μL) for 5 mL of M9 media (pH 5.7, 6.5, and 7.5). Cultures were incubated at 37 °C, aliquots of 200 μL were collected at various time points and centrifuged, and the supernatant was analyzed by LC-MS.

■ ASSOCIATED CONTENT

Supporting Information

The Supporting Information is available free of charge on the ACS Publications website at DOI: 10.1021/acsinfecdis.5b00145.

Synthesis of benzyl pre-acinetobactin **12**, compound characterization data (NMR, CD, UV−vis, LC-MS, high-res MS−MS), and *A. baumannii* growth curves (PDF)

■ AUTHOR INFORMATION

Corresponding Author

*E-mail: wencewicz@wustl.edu. Phone: 314-935-7247. Fax: 314-935-6530.

Notes

The authors declare no competing financial interest.

■ ACKNOWLEDGMENTS

We thank A. D'Avignon (formerly WUSTL, Department of Chemistry; currently Sanford Burnham Medical Research Institute, Orlando, FL), J. Kao (WUSTL, Department of Chemistry), and B. Marsden (WUSTL, Department of Chemistry) for assistance in the acquisition of 2D NMR spectra. We thank C. Frieden and Q. Shu (WUSTL School of Medicine, Department of Biochemistry and Molecular Biophysics) for assistance with CD measurements. We thank S. Alvarez at the Proteomics & Mass Spectrometry Facility at the Donald Danforth Plant Science Center, St. Louis, MO, for assistance with the acquisition of high-resolution MS−MS spectra (Grant No. DBI-0922879). A special thanks to Dr. Luis Actis (Miami University, Department of Microbiology) for providing *A. baumannii* ATCC 19606 t6, t7, and s1 mutants. Research was supported by Oak Ridge Associated Universities through a Ralph E. Powe Junior Faculty Enhancement Award (FY2014-215) and by funds from Washington University in St. Louis.

■ ABBREVIATIONS

A. baumannii, *Acinetobacter baumannii*; CD, circular dichroism; D_2O, deuterium oxide; DCE, 1,2-dichloroethane; EIC, extracted ion chromatogram; ESI, electrospray ionization; HEPES, 2-[4-(2-hydroxyethyl)piperazin-1-yl]ethanesulfonic acid; HPLC, high performance liquid chromatography; HRMS, high-resolution mass spectrometry; LB, lysogeny broth; LC-MS, liquid chromatography−mass spectrometry; MRSA, methicillin-resistant *Staphylococcus aureus*; NMR, nuclear magnetic resonance; OD, optical density; rpm, rotations per minute; Tris, 2-amino-2-hydroxymethylpropane-1,3-diol; TFA, trifluoroacetic acid

■ REFERENCES

(1) Peleg, A. Y., and Hooper, D. C. (2010) Hospital-acquired infections due to Gram-negative bacteria. *N. Engl. J. Med. 362*, 1804.

(2) Peleg, A. Y., Seifert, H., and Paterson, D. L. (2008) *Acinetobacter baumannii*: emergence of a successful pathogen. *Clin. Microbiol. Rev. 21*, 538.

(3) *Antibiotic Resistance Threats in the United States, 2013*; Center for Disease Control and Prevention, U.S. Department of Health and Human Services: Washington DC, Published Online, 2013.

(4) Zhou, H., Zhang, T., Yu, D., Pi, B., Yang, Q., Zhou, J., Hu, S., and Yu, Y. (2011) Genomic analysis of the multidrug-resistant *Acinetobacter baumannii* strain MDR-ZJ06 widely spread in China. *Antimicrob. Agents Chemother. 55*, 4506.

DOI: 10.1021/acsinfecdis.5b00145
ACS Infect. Dis. 2016, 2, 157−168

(5) Landman, D., Georgescu, C., Martin, D. A., and Quale, J. (2008) Polymyxins revisited. *Clin. Microbiol. Rev. 21*, 449.
(6) Lood, R., Winer, B. Y., Pelzek, A. J., Diez-Martinez, R., Thandar, M., Euler, C. W., Schuch, R., and Fischetti, V. A. (2015) Novel phage lysin capable of killing the multidrug-resistant gram-negative bacterium *Acinetobacter baumannii* in a mouse bacteremia model. *Antimicrob. Agents Chemother. 59*, 1983.
(7) Antunes, L. C. S., Imperi, F., Carattoli, A., and Visca, P. (2011) Deciphering the Multifactorial Nature of *Acinetobacter baumannii* Pathogenicity. *PLoS One 6*, e22674.
(8) Eijkelkamp, B. A., Hassan, K. A., Paulsen, I. T., and Brown, M. H. (2011) Investigation of the human pathogen *Acinetobacter baumannii* under iron limiting conditions. *BMC Genomics 12*, 126.
(9) Mortensen, B. L., and Skaar, E. P. (2013) The contribution of nutrient metal acquisition and metabolism to *Acinetobacter baumannii* survival within the host. *Front. Cell. Infect. Microbiol. 3*, 95.
(10) Neres, J., Engelhart, C. A., Drake, E. J., Wilson, D. J., Fu, P., Boshoff, H. I., Barry, C. E., 3rd, Gulick, A. M., and Aldrich, C. C. (2013) Non-nucleoside Inhibitors of BasE, An Adenylating Enzyme in the Siderophore Biosynthetic Pathway of the Opportunistic Pathogen *Acinetobacter baumannii*. *J. Med. Chem. 56*, 2385.
(11) Antunes, L. C., Imperi, F., Towner, K. J., and Visca, P. (2011) Genome-assisted identification of putative iron-utilization genes in *Acinetobacter baumannii* and their distribution among a genotypically diverse collection of clinical isolates. *Res. Microbiol. 162*, 279.
(12) Ratledge, C., and Dover, L. G. (2000) Iron metabolism in pathogenic bacteria. *Annu. Rev. Microbiol. 54*, 881.
(13) Neilands, J. B. (1995) Siderophores: structure and function of microbial iron transport compounds. *J. Biol. Chem. 270*, 26723.
(14) Schaible, U. E., and Kaufmann, S. H. (2004) Iron and microbial infection. *Nat. Rev. Microbiol. 2*, 946.
(15) Miethke, M., and Marahiel, M. A. (2007) Siderophore-based iron acquisition and pathogen control. *Microbiol. Mol. Biol. Rev. 71*, 413.
(16) Yamamoto, S., Okujo, N., and Sakakibara, Y. (1994) Isolation and structure elucidation of acinetobactin, a novel siderophore from *Acinetobacter baumannii*. *Arch. Microbiol. 162*, 249.
(17) Proschak, A., Lubuta, P., Grun, P., Lohr, F., Wilharm, G., De Berardinis, V., and Bode, H. B. (2013) Structure and biosynthesis of fimsbactins A-F, siderophores from *Acinetobacter baumannii* and Acinetobacter baylyi. *ChemBioChem 14*, 633.
(18) Penwell, W. F., DeGrace, N., Tentarelli, S., Gauthier, L., Gilbert, C. M., Arivett, B. A., Miller, A. A., Durand-Reville, T. F., Joubran, C., and Actis, L. A. (2015) Discovery and Characterization of New Hydroxamate Siderophores, Baumannoferrin A and B, produced by *Acinetobacter baumannii*. *ChemBioChem 16*, 1896.
(19) Gaddy, J. A., Arivett, B. A., McConnell, M. J., Lopez-Rojas, R., Pachon, J., and Actis, L. A. (2012) Role of acinetobactin-mediated iron acquisition functions in the interaction of *Acinetobacter baumannii* strain ATCC 19606T with human lung epithelial cells, *Galleria mellonella* caterpillars, and mice. *Infect. Immun. 80*, 1015.
(20) Hasan, T., Choi, C. H., and Oh, M. H. (2015) Genes Involved in the Biosynthesis and Transport of Acinetobactin in *Acinetobacter baumannii*. *Genomics Inform. 13*, 2.
(21) Mihara, K., Tanabe, T., Yamakawa, Y., Funahashi, T., Nakao, H., Narimatsu, S., and Yamamoto, S. (2004) Identification and transcriptional organization of a gene cluster involved in biosynthesis and transport of acinetobactin, a siderophore produced by *Acinetobacter baumannii* ATCC 19606T. *Microbiology (London, U. K.) 150*, 2587.
(22) Dorsey, C. W., Tomaras, A. P., Connerly, P. L., Tolmasky, M. E., Crosa, J. H., and Actis, L. A. (2004) The siderophore-mediated iron acquisition systems of *Acinetobacter baumannii* ATCC 19606 and Vibrio anguillarum 775 are structurally and functionally related. *Microbiology 150*, 3657.
(23) Sattely, E. S., and Walsh, C. T. (2008) A latent oxazoline electrophile for N-O-C bond formation in pseudomonine biosynthesis. *J. Am. Chem. Soc. 130*, 12282.
(24) Wuest, W. M., Sattely, E. S., and Walsh, C. T. (2009) Three siderophores from one bacterial enzymatic assembly line. *J. Am. Chem. Soc. 131*, 5056.
(25) Penwell, W. F., Arivett, B. A., and Actis, L. A. (2012) The *Acinetobacter baumannii* entA Gene Located Outside the Acinetobactin Cluster Is Critical for Siderophore Production, Iron Acquisition and Virulence. *PLoS One 7*, e36493.
(26) Drake, E. J., Duckworth, B. P., Neres, J., Aldrich, C. C., and Gulick, A. M. (2010) Biochemical and structural characterization of bisubstrate inhibitors of BasE, the self-standing nonribosomal peptide synthetase adenylate-forming enzyme of acinetobactin synthesis. *Biochemistry 49*, 9292.
(27) Anthoni, U., Christophersen, C., Nielsen, P. H., Gram, L., and Petersen, B. O. (1995) Pseudomonine, an isoxazolidone with siderophoric activity from *Pseudomonas fluorescens* AH2 isolated from Lake Victorian Nile perch. *J. Nat. Prod. 58*, 1786.
(28) Actis, L. A., Fish, W., Crosa, J. H., Kellerman, K., Ellenberger, S. R., Hauser, F. M., and Sanders-Loehr, J. (1986) Characterization of anguibactin, a novel siderophore from *Vibrio anguillarum* 775(pJM1). *J. Bacteriol. 167*, 57.
(29) Naka, H., Liu, M., Actis, L. A., and Crosa, J. H. (2013) Plasmid- and chromosome-encoded siderophore anguibactin systems found in marine vibrios: biosynthesis, transport and evolution. *BioMetals 26*, 537.
(30) Jalal, M. A. F., Hossain, M. B., Van der Helm, D., Sanders-Loehr, J., Actis, L. A., and Crosa, J. H. (1989) Structure of anguibactin, a unique plasmid-related bacterial siderophore from the fish pathogen *Vibrio anguillarum*. *J. Am. Chem. Soc. 111*, 292.
(31) Higgins, P. G., Stubbings, W., Wisplinghoff, H., and Seifert, H. (2010) Activity of the investigational fluoroquinolone finafloxacin against ciprofloxacin-sensitive and -resistant *Acinetobacter baumannii* isolates. *Antimicrob. Agents Chemother. 54*, 1613.
(32) Takeuchi, Y., Ozaki, S., Satoh, M., Mimura, K., Hara, S., Abe, H., Nishioka, H., and Harayama, T. (2010) Synthesis of acinetobactin. *Chem. Pharm. Bull. 58*, 1552.
(33) Baldwin, J. (1976) Rules for ring closure. *J. Chem. Soc., Chem. Commun.*, 734−736.
(34) Hider, R. C., and Kong, X. (2010) Chemistry and biology of siderophores. *Nat. Prod. Rep. 27*, 637.
(35) Allred, B. E., Correnti, C., Clifton, M. C., Strong, R. K., and Raymond, K. N. (2013) Siderocalin outwits the coordination chemistry of vibriobactin, a siderophore of *Vibrio cholerae*. *ACS Chem. Biol. 8*, 1882.
(36) Bao, G., et al. (2010) Iron traffics in circulation bound to a siderocalin (Ngal)-catechol comple. *Nat. Chem. Biol. 6* (8), 602.
(37) Raymond, K. N., Allred, B. E., and Sia, A. K. (2015) Coordination Chemistry of Microbial Iron Transport. *Acc. Chem. Res. 48*, 2496.
(38) Henderson, J. P., Crowley, J. R., Pinkner, J. S., Walker, J. N., Tsukayama, P., Stamm, W. E., Hooton, T. M., and Hultgren, S. J. (2009) Quantitative metabolomics reveals an epigenetic blueprint for iron acquisition in uropathogenic *Escherichia coli*. *PLoS Pathog. 5*, e1000305.
(39) Shields-Cutler, R. R., Crowley, J. R., Hung, C. S., Stapleton, A. E., Aldrich, C. C., Marschall, J., and Henderson, J. P. (2015) Human urinary composition controls siderocalin's antibacterial activity. *J. Biol. Chem. 290*, 15949.
(40) Ymamoto, S., Okujo, N., Kataoka, H., and Narimatsu, S. (1999) Siderophore-mediated utilization of transferrin- and lactoferrin-bound iron by *Acinetobacter baumannii*. *J. Health Sci. 45*, 297.
(41) Koh, E. I., and Henderson, J. P. (2015) Microbial Copper-binding Siderophores at the Host-Pathogen Interface. *J. Biol. Chem. 290*, 18967.
(42) Okujo, N., Sakakibara, Y., Yoshida, T., and Yamamoto, S. (1994) Structure of acinetoferrin, a new citrate-based dihydroxamate siderophore from *Acinetobacter haemolyticus*. *BioMetals 7*, 170.
(43) Luo, M., Fadeev, E. A., and Groves, J. T. (2005) Membrane dynamics of the amphiphilic siderophore, acinetoferrin. *J. Am. Chem. Soc. 127*, 1726.

DOI: 10.1021/acsinfecdis.5b00145
ACS Infect. Dis. 2016, 2, 157−168

(44) Funahashi, T., Tanabe, T., Mihara, K., Miyamoto, K., Tsujibo, H., and Yamamoto, S. (2012) Identification and characterization of an outer membrane receptor gene in *Acinetobacter baumannii* required for utilization of desferricoprogen, rhodotorulic acid, and desferrioxamine B as xenosiderophores. *Biol. Pharm. Bull. 35*, 753.
(45) Madsen, J. L., Johnstone, T. C., and Nolan, E. M. (2015) Chemical Synthesis of Staphyloferrin B Affords Insight into the Molecular Structure, Iron Chelation, and Biological Activity of a Polycarboxylate Siderophore Deployed by the Human Pathogen *Staphylococcus aureus*. *J. Am. Chem. Soc. 137*, 9117.
(46) Wencewicz, T. A., Mollmann, U., Long, T. E., and Miller, M. J. (2009) Is drug release necessary for antimicrobial activity of siderophore-drug conjugates? Syntheses and biological studies of the naturally occurring salmycin ″Trojan Horse″ antibiotics and synthetic desferridanoxamine-antibiotic conjugates. *BioMetals 22*, 633.
(47) Zheng, T., and Nolan, E. M. (2014) Enterobactin-Mediated Delivery of β-Lactam Antibiotics Enhances Antibacterial Activity against Pathogenic *Escherichia coli*. *J. Am. Chem. Soc. 136*, 9677.
(48) Ross-Gillespie, A., Weigert, M., Brown, S. P., and Kümmerli, R. (2014) Gallium-mediated siderophore quenching as an evolutionarily robust antibacterial treatment. *Evol. Med. Public Health 2014*, 18.
(49) Thornton, A. B., Thomson, D. U., Loneragan, G. H., Fox, J. T., Burkhardt, D. T., Emery, D. A., and Nagaraja, T. G. (2009) Effects of a siderophore receptor and porin proteins-based vaccination on fecal shedding of *Escherichia coli* O157:H7 in experimentally inoculated cattle. *J. Food Protect. 72*, 866.
(50) Petrik, M., Franssen, G. M., Haas, H., Laverman, P., Hortnagl, C., Schrettl, M., Helbok, A., Lass-Florl, C., and Decristoforo, C. (2012) Preclinical evaluation of two 68Ga-siderophores as potential radiopharmaceuticals for *Aspergillus fumigatus* infection imaging. *Eur. J. Nucl. Med. Mol. Imaging 39*, 1175.
(51) Zheng, T., Bullock, J. L., and Nolan, E. M. (2012) Siderophore-mediated cargo delivery to the cytoplasm of *Escherichia coli* and *Pseudomonas aeruginosa*: syntheses of monofunctionalized enterobactin scaffolds and evaluation of enterobactin-cargo conjugate uptake. *J. Am. Chem. Soc. 134*, 18388.
(52) Johnstone, T. C., and Nolan, E. M. (2015) Beyond iron: non-classical biological functions of bacterial siderophores. *Dalton Trans. 44*, 6320.
(53) Murray, P. R.; Baron, E. J.; Pfaller, M. A.; Tenover, F. C.; Yolken, R. H. (1996) *Manual of Clinical Microbiology*, 7th ed.; American Society for Microbiology: Washington, DC.

DOI: 10.1021/acsinfecdis.5b00145
ACS Infect. Dis. 2016, 2, 157−168